

## Cyclopropyl Conjugation and Ketyl Anions: When Do Things Begin to Fall Apart?

J. M. Tanko,\* Xiangzhong Li, M'hamed Chahma, Woodward F. Jackson, and Jared N. Spencer

Department of Chemistry, Virginia Polytechnic Institute and State University,  
Blacksburg, Virginia 24061

Received June 1, 2006; E-mail: jtanko@vt.edu

**Abstract:** Results pertaining to the electrochemical reduction of 1,2-diacetylcyclopropane (**5**), 1-acetyl-2-phenylcyclopropane (**6**), 1-acetyl-2-benzoylcyclopropane (**7**), and 1,2-dibenzoylcyclopropane (**8**) are reported. While **6**<sup>•-</sup> exists as a discrete species, the barrier to ring opening is very small (<1 kcal/mol) and the rate constant for ring opening is >10<sup>7</sup> s<sup>-1</sup>. For **7** and **8**, the additional resonance stabilization afforded by the benzoyl moieties results in significantly lower rate constants for ring opening, on the order of 10<sup>5</sup>–10<sup>6</sup> s<sup>-1</sup>. Electron transfer to **8** serves to initiate an unexpected vinylcyclopropane → cyclopentene type rearrangement, which occurs via a radical ion chain mechanism. The results for reduction of **5** are less clear-cut: The experimental results suggest that the reduction is unexceptional, with a symmetry coefficient  $\alpha \leq 0.5$ , and reorganization energy consistent with a simple electron-transfer process (one electron reduction, followed by ring opening). In contrast, molecular orbital calculations suggest that **5**<sup>•-</sup> has no apparent lifetime and that reduction of **5** may occur by a concerted dissociative electron transfer (DET) mechanism (i.e., electron transfer and ring opening occur simultaneously). These seemingly contradictory results can be reconciled if the increase in the internal reorganization energy associated with the onset of concerted DET is offset by a lowering of the solvent reorganization energy associated with electron transfer to a more highly delocalized LUMO.

### Introduction

Cyclopropyl groups are unique as alkyl substituents because of their characteristic bonding features. The Walsh/Sugden model<sup>1–3</sup> constructs cyclopropane from three sp<sup>2</sup>-hybridized CH<sub>2</sub> fragments, with the sp<sup>2</sup> hybrid orbitals oriented radially toward the center of the three membered ring, and the three p orbitals coplanar (constituting a Hückel and Möbius array, respectively). The HOMO and LUMO for cyclopropane arise from the latter and are depicted in Figure 1. The theoretical foundation for the cyclopropyl group as a good  $\pi$ -electron donor is well established and attributable to interaction of one of the degenerate cyclopropyl HOMOs ( $\psi_1$ ) with an adjacent  $\pi$  system; this interaction is maximal in the so-called bisected conformation, where the cyclopropyl p-derived orbitals are fully aligned with the  $\pi$  system.<sup>4,5</sup> As a result of  $\pi$ -donation, the cyclopropyl group stabilizes electron-deficient species such as free radicals<sup>6</sup> and carbocations.<sup>7</sup> For other  $\pi$  systems (e.g., carbonyl, vinyl, phenyl), interactions with the cyclopropyl group have been detected by predictable geometric distortions measured by X-ray crystallography,<sup>8</sup> chemical shift changes measured by NMR, and perturbations detected by other forms of spectroscopy.<sup>7</sup>

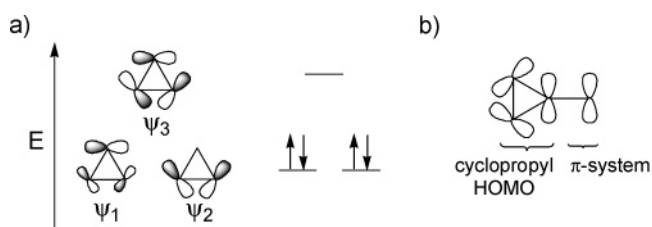


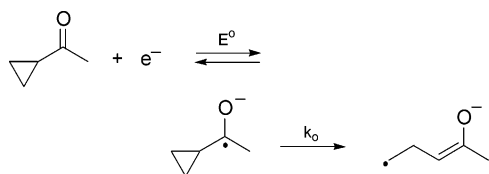
**Figure 1.** Depiction of (a) the p-derived molecular orbitals of cyclopropane and (b) the interaction of the cyclopropyl HOMO with an adjacent  $\pi$  system in the bisected conformation.

The ability of the cyclopropyl group to act as a  $\pi$ -electron acceptor to stabilize an electron-rich center is less clear-cut. Experimental evidence has been presented which suggests the cyclopropyl group can stabilize a negative charge in some cases,<sup>9</sup> but the effect is not general.<sup>7</sup> In an electrochemical approach to the question, the cyclopropyl group was reported to have no discernible effect on the half-wave (reduction) potentials of activated olefins.<sup>10</sup> Clark and Schleyer have concluded that the cyclopropyl group can act as either a  $\sigma$ - or  $\pi$ -acceptor only in extreme cases (i.e., with potent electron donors), invoking a slightly more complicated molecular orbital description of the Walsh model than presented here.<sup>11</sup>

(1) Sugden, T. M. *Nature (London)* **1947**, *160*, 367–268.  
 (2) Walsh, A. D. *Nature (London)* **1947**, *159*, 712–713.  
 (3) Walsh, A. D. *Trans. Faraday Soc.* **1949**, *54*, 179–190.  
 (4) Hoffmann, R.; Davidson, R. B. *J. Am. Chem. Soc.* **1971**, *93*, 5699–5704.  
 (5) Wiberg, K. B. *Acc. Chem. Res.* **1996**, *29*, 229–234.  
 (6) Walton, J. C. *Magn. Reson. Chem.* **1987**, *25*, 998–1000.  
 (7) Tidwell, T. T. In *The Chemistry of the Cyclopropyl Group*; Rappoport, Z., Ed.; John Wiley and Sons: New York, 1987; pp 565–632.

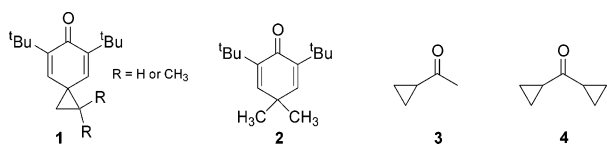
(8) Allen, F. H. *Acta Crystallogr.* **1980**, *B 36*, 81–96.  
 (9) Perkins, M. J.; Peynircioglu, N. B. *Tetrahedron* **1985**, *41*, 225–227.  
 (10) Baizer, M. M.; Chruma, J. L.; Berger, P. A. *J. Org. Chem.* **1970**, *35*, 3569–3571.

Scheme 1

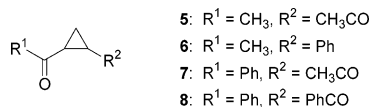


Our group has been interested in the electrochemistry of cyclopropyl ketones, particularly with regard to the rate constants for ring opening of their corresponding radical anions (Scheme 1).<sup>12–20</sup> Although the emphasis of these studies has been on the ring-opening reaction, we have collected a fair amount of thermodynamic data pertaining to the issue of the cyclopropyl group as a substituent and its ability to stabilize a ketyl anion. Specifically, these experiments have led to good estimates of the reduction potentials of several cyclopropyl-containing carbonyl compounds. The fast cyclopropane ring opening of many of these radical anions enables the use of an electrochemical method (homogeneous redox catalysis, *vide infra*) which allows measurement of the reduction potentials of some classes of compounds (e.g., aliphatic ketones) which could not be measured otherwise.<sup>12–14,19</sup>

To date, we have found no evidence that the cyclopropyl group can significantly affect the reduction potential of a ketone or stabilize a radical anion. For example, spiro[2.5]octa-4,7-dien-6-ones **1** have nearly the same reduction potential as cyclohexadienone **2**.<sup>13</sup> Similarly, within experimental error, methyl cyclopropyl ketone (**3**) and dicyclopropyl ketone (**4**) have the same reduction potential.<sup>14,19</sup>



In this paper, we report our results pertaining to the electrochemical reduction of substituted cyclopropyl ketones **5** → **8**.



## Experimental Section

**Materials.** *N,N*-Dimethylformamide (DMF, EM Science, 98%) was stirred over copper(II) sulfate (Aldrich, 98%) and activated alumina (Aldrich, neutral, Brockman activity 1) for >3 days and vacuum-distilled immediately before use. Alumina was flame-dried under

vacuum (until evolution of water vapor ceased) prior to use. Tetra-*n*-butylammonium perchlorate (TBAP) was prepared by the method of House<sup>21</sup> and recrystallized 4× from ethyl acetate/hexane and vacuum-oven-dried before use. 1,2-Diacetylcyclopropane (**5**),<sup>22</sup> 2-phenyl-1-acetylcyclopropane (**6**),<sup>23</sup> and 2-benzoyl-1-acetylcyclopropane (**7**)<sup>24</sup> (all mainly *trans*) were prepared according to published procedures. *trans*-1,2-Dibenzoylcyclopropane (**8**) and all of the mediators used in this study were obtained from Aldrich.

**General.** GC/MS was performed on a Hewlett-Packard HP 5890 gas chromatograph interfaced to a HP 5970 low-resolution mass spectrometer and a HP series computer. High-resolution mass spectral data were obtained from a VG Analytical model 7070 E-HF double-focusing magnetic sector high-resolution spectrometer using electron impact (70 eV) ionization. GC analysis was performed on a Hewlett-Packard 5890A gas chromatograph equipped with an FID detector and an HP 3393A reporting integrator. Nuclear magnetic resonance spectra (<sup>1</sup>H, <sup>13</sup>C) were obtained on either a Bruker WP 270 MHz, Bruker AM 360 MHz, or a Varian Unity 400 MHz FT NMR spectrometer. Infrared spectra were recorded on a Perkin-Elmer model 1600 FT-IR spectrometer. Molecular orbital calculations were performed using Gaussian 03<sup>25</sup> (running on SGI Inferno 2, a super-cluster containing 64 1.6 GHz Itanium 2 processors and 256 GB of memory) and/or Spartan '04<sup>26</sup> (running on a Windows XP system with an AMD 1.8 GHz XP2200+ processor and 2 GB of RAM).

**Electrochemistry.** Electrochemical measurements were performed on an EG&G Princeton Applied Research (EG&G/PAR) model 273 potentiostat/galvanostat interfaced to an MS-DOS computer. The details of this system were described earlier.<sup>13,14,17</sup> Briefly, a three-electrode voltammetry cell was used with a glassy carbon working electrode (GCE), which was fabricated from 0.5 cm diameter glassy carbon rod (type 1, Alfa Aesar). The GC rod was cut into several 4–5 mm plugs, which were secured into glass rods with Torrseal-Varian vacuum epoxy resin (Varian vacuum products), and attached to a Cu brazing rod with silver two-part conductive adhesive (Alfa Aesar). After being sanded, the electrode surface was polished with alumina slurry (Buehler) starting with 1.0 μm grit and decreasing to 0.3 and finally 0.05 μm until a mirror finish was obtained. The area was 0.197 cm<sup>2</sup>, determined from the voltammetric response of ferrocene whose diffusion coefficient in 0.1 M TBAP/DMF is known.<sup>27</sup> The reference electrode was Ag/AgNO<sub>3</sub> (0.1 M in CH<sub>3</sub>CN, 0.337 V vs SCE). For calibration purposes, ferrocene oxidation occurs at +0.035 V in DMF versus this reference electrode. A Pt wire coil was used as the auxiliary electrode. Positive-feedback IR compensation was employed.

The following protocol was followed for the voltammetry experiments: After the working electrode was thoroughly polished with fine alumina (0.05 μm), it was subsequently rinsed with isopropyl alcohol and sonicated for 15 min (to remove any residual alumina from the surface). The electrode was activated by scanning over the potential range several times at 100 mV/s, and then background voltammograms (solvent + electrolyte—no substrate) were obtained. Adsorption of the products formed during the reduction was a problem for all the substrates, and it was usually necessary to repeat this cleansing process between runs.

Preparative-scale electrolyses were performed on solutions which contained 0.2 M TBAP in DMF. A conventional H-cell with two compartments separated by a medium glass frit was utilized. A gold foil working electrode (4 cm<sup>2</sup>) was utilized. All electrolysis experiments were performed at ambient temperature. Reaction progress was

- (11) Clark, T.; Spitzmagel, G. W.; Klose, R.; Schleyer, P. v. R. *J. Am. Chem. Soc.* **1984**, *106*, 4412–4419.  
 (12) Chahma, M.; Li, X.; Phillips, J. P.; Schwartz, P.; Brammer, L. E.; Wang, Y.; Tanko, J. M. *J. Phys. Chem. A* **2005**, *109*, 3372–3382.  
 (13) Phillips, J. P.; Gillmore, J. G.; Schwartz, P.; Brammer, L. E., Jr.; Berger, D. J.; Tanko, J. M. *J. Am. Chem. Soc.* **1998**, *120*, 195–202.  
 (14) Stevenson, J. P.; Jackson, W. F.; Tanko, J. M. *J. Am. Chem. Soc.* **2002**, *124*, 4271–4281.  
 (15) Tanko, J. M.; Brammer, L. E., Jr.; Hervas, M.; Campos, K. *J. Chem. Soc. Perkin Trans. 2* **1994**, 1407–1409.  
 (16) Tanko, J. M.; Drumright, R. E. *J. Am. Chem. Soc.* **1990**, *112*, 5362–5363.  
 (17) Tanko, J. M.; Drumright, R. E. *J. Am. Chem. Soc.* **1992**, *114*, 1844–1854.  
 (18) Tanko, J. M.; Drumright, R. E.; Suleman, N. K.; Brammer, L. E., Jr. *J. Am. Chem. Soc.* **1994**, *116*, 1785–1791.  
 (19) Tanko, J. M.; Phillips, J. P. *J. Am. Chem. Soc.* **1999**, *121*, 6078–6079.  
 (20) Tanko, J. M.; Gillmore, J. G.; Friedline, R.; Chahma, M. *J. Org. Chem.* **2005**, *70*, 4170–4173.

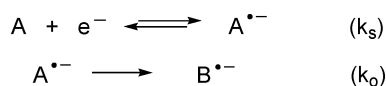
- (21) House, H. O.; Feng, E.; Pert, N. P. *J. Org. Chem.* **1971**, *36*, 2371–2375.  
 (22) Maier, G.; Sayrac, T. *Chem. Ber.* **1968**, *101*, 1354–1370.  
 (23) DePuy, C. H.; Dappen, G. M.; Eilers, K. L.; Klein, R. A. *J. Org. Chem.* **1964**, *29*, 2813–2815.  
 (24) Doyle, M. P.; Buhro, W. E.; Dellaria, J. F. *Tetrahedron Lett.* **1979**, *46*, 4429–4432.  
 (25) Frisch, M. J.; et al. *Gaussian 03, Revision C.02*.  
 (26) *Spartan '04*; Wavefunction, Inc.: Irvine, CA, 2004.  
 (27) Jacob, S. R.; Hong, Q.; Coles, B. A.; Compton, R. G. *J. Phys. Chem. B* **1999**, *103*, 2963–2969.

monitored by GC where necessary. Solution workup consisted of quenching the cathodic compartment with 1 mL of 5% H<sub>2</sub>SO<sub>4</sub>, adding 50 mL of water, and extracting with 4 × 50 mL of ether. Ether layers were combined, washed with water, washed with saturated NaCl solution, dried over MgSO<sub>4</sub>, and concentrated. Products of bulk electrolysis were all known compounds. Yields were determined by GC vs an appropriate internal standard; mass balances were ca. 90%.

## Results

**Direct Electrochemistry.** With direct electrochemical techniques<sup>28–31</sup> such as cyclic and linear sweep voltammetry (CV and LSV, respectively), substrate **A** (Scheme 2) is reduced at an electrode surface generating radical anion **A**<sup>•−</sup>; *k*<sub>S</sub> represents the standard heterogeneous rate constant for this step (rate constant when Δ*G*<sup>o</sup> = 0). This radical anion undergoes subsequent ring opening yielding **B**<sup>•−</sup> with rate constant *k*<sub>o</sub>. Either of these steps may be rate-limiting, depending on the nature of the substrate. Kinetic data are obtained by examining the effect of sweep rate and substrate concentration on the electrochemical response. When the chemical step is rate-limiting, it is possible to obtain information such as the formal reduction potential of the substrate (*E*<sup>o</sup><sub>A/A<sup>•−</sup>), the rate law for the chemical step, and the rate constant *k*<sub>o</sub>. When heterogeneous electron transfer is rate-limiting, it is possible to measure *k*<sub>S</sub> and the electron-transfer coefficient α. The value of α is a measure of transition state location, and can be used to distinguish between stepwise and dissociative electron transfer (DET, vide infra).</sub>

### Scheme 2



For systems whose kinetics were electron-transfer-controlled, the voltammograms were further subjected to convolution analysis.<sup>32</sup> In this treatment, a convolution voltammogram (plot of *I*(*t*) vs *E*) is generated in accordance with eq 1, where *I*(*t*) and *i*(*t*) are the convolutive and “normal” currents at time *t*. The limiting convolutive current, *I*<sub>lim</sub>, is independent of sweep rate, eq 2 (where *n*, *F*, *A*, *D*, and *C* have their usual meanings). Convolution voltammograms were generated by numerical integration of the original voltammograms using a simple BASIC program written in-house. Convolution voltammograms for **5** and **6** are provided in the Supporting Information.

$$I(t) = \frac{1}{\pi^{1/2}} \int_0^t \frac{i(u)}{(t-u)^{1/2}} du \quad (1)$$

$$I_{\text{lim}} = nFAD^{1/2}C \quad (2)$$

The convolution approach essentially eliminates the mass transport component of the electrochemical response and, in principle, allows all the data associated with the voltammogram to be analyzed, as opposed to relying on single-point measure-

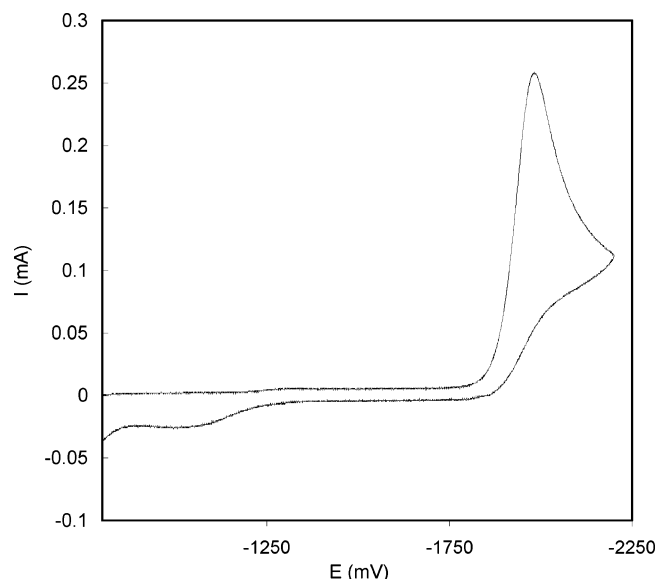


**Figure 2.** Cyclic voltammogram of 1,2-dibenzoylcyclopropane (**8**, 0.0020 M in 0.5 M *n*-Bu<sub>4</sub>NClO<sub>4</sub>/DMF) at 100 mV/s.

ments such as the peak or half-peak potential. This method is particularly useful when electron transfer is rate-limiting. A plot of *E* vs the current function ln(*I*<sub>lim</sub> − *I*(*t*)/*i*(*t*)) permits the standard heterogeneous rate constant (*k*<sub>S</sub>) and the average value of the transfer coefficient α to be determined (eq 3, assuming Butler–Volmer kinetics); through eq 4, the potential dependent heterogeneous rate constant (*k*<sub>het</sub>) can be calculated at any point on the voltammogram (without the Butler–Volmer assumption), and via differentiation (eq 5), the potential dependence of α can be determined.<sup>33</sup> (Note: Because the current function becomes noisy at the extremes *i*(*t*) → 0 and *I*(*t*) → *I*<sub>lim</sub>, only data in the 10–90% range of *I*<sub>lim</sub> were used in these analyses.)

$$E = E^o - \frac{RT}{\alpha nF} \ln\left(\frac{D^{1/2}}{k_S}\right) + \frac{RT}{\alpha nF} \ln\left(\frac{I_{\text{lim}} - I(t)}{i(t)}\right) \quad (3)$$

$$\ln(k_{\text{het}}) = \ln(D)^{1/2} - \ln\left(\frac{I_{\text{lim}} - I(t)}{i(t)}\right) \quad (4)$$

$$\alpha = \frac{\partial \Delta G^\ddagger}{\partial \Delta G^o} = -\left(\frac{RT}{F}\right) \frac{\partial \ln k_{\text{het}}}{\partial E} \quad (5)$$

Cyclic voltammograms for compounds **5–8** all exhibit the following characteristics: For each substrate, the reduction wave is not accompanied by a corresponding oxidation wave (at scan rates up to 100 V/s), consistent with the expectation that cyclopropane ring opening occurs rapidly on the time scale of these experiments. An oxidation wave observed at −600 → −1200 mV is attributed to oxidation of an enolate anion<sup>34</sup> which results from the ring-opening reaction. (For a representative voltammogram, see Figure 2). In each case, the magnitude of the peak current is consistent with a two-electron reduction, based upon *I*<sub>lim</sub> (eq 2) and estimates of the diffusion coefficient based on molecules of similar size. Because these voltammograms are irreversible, any mechanistic and kinetic inferences

(28) Amatore, C.; Savéant, J. M. *J. Electroanal. Chem.* **1977**, *85*, 27–46.

(29) Andrieux, C. P.; Savéant, J. M. In *Investigation of Rates and Mechanisms of Reactions. Part II*, 4th ed.; Bernasconi, C., Ed.; Wiley: New York, 1986; pp 305–390.

(30) Nadjo, L.; Savéant, J. M. *Electroanal. Chem.* **1973**, *48*, 113–145.

(31) Parker, V. D. In *Electrode kinetics: Principles and methodology*; Bamford, C. H., Compton, R. G., Eds. Elsevier: Amsterdam, 1986; Vol. 26, pp 145–202.

(32) Imbeaux, J. C.; Savéant, J.-M. *J. Electroanal. Chem.* **1973**, *44*, 169–187.

(33) Bard, A. J.; Faulkner, L. R.; Wiley: New York, 1980, p 236–243.

(34) Daasbjerg, K.; Pedersen, S. U.; Lund, H. In *General Aspects of the Chemistry of Radicals*; Alfassi, Z. B., Ed.; Wiley: Chichester, UK, 1999; pp 385–427.



**Table 1.** LSV Data for Compounds 5–8

compound	$\partial E_p/\partial \log \nu$ (mV/decade) <sup>a</sup>	$ E_p - E_{p/2} $ (mV)	$\alpha$
<b>5</b>	-64	119	0.46, <sup>b</sup> 0.40, <sup>c</sup> 0.43 <sup>d</sup>
<b>6</b>	-57	104	0.51, <sup>b</sup> 0.46, <sup>c</sup> 0.49 <sup>d</sup>
<b>7</b>	-42	72–90 <sup>e</sup>	0.5 <sup>f</sup>
<b>8</b>	-40	54–80 <sup>e</sup>	0.5 <sup>f</sup>

<sup>a</sup>  $\partial E_p/\partial \log C_A \approx 0$ . <sup>b</sup> Calculated from  $\partial E_p/\partial \log \nu$ . <sup>c</sup> Calculated from  $E_p - E_{p/2}$ . <sup>d</sup> Obtained from convolution analysis (eq 3). <sup>e</sup> Increases steadily with increasing sweep rate. <sup>f</sup> Assumed.

are based upon the peak potential ( $E_p$ ) and peak width (the difference between the peak and half-peak potential,  $E_p - E_{p/2}$ .)

If the chemical step (ring opening) is rate limiting, the expected variation of  $E_p$  with sweep rate ( $\nu$ ) and concentration ( $C_A$ ) are  $\partial E_p/\partial \log \nu = -29.6$  and  $\partial E_p/\partial \log C_A = 0$  mV/decade. The peak width,  $E_p - E_{p/2}$ , is expected to be around 50 mV and invariant with sweep rate. In contrast, if electron transfer is rate-limiting,  $\partial E_p/\partial \log \nu = -29.6/\alpha$  and  $\partial E_p/\partial \log C_A = 0$  mV/decade, where  $\alpha$  is the transfer coefficient discussed above. Another characteristic feature of rate-limiting electron transfer is that the peak widths are notably greater than 50 mV, with  $E_p - E_{p/2} = 1.85RT/\alpha F$ .<sup>30</sup>

For all the compounds studied,  $E_p$  did not vary significantly with substrate concentration; the other significant features of the voltammetry are summarized in Table 1; representative voltammograms are provided in the Supporting Information.

Compounds **5** and **6** are clearly in the regime where the kinetics is governed by electron transfer. For each compound, the calculated (average) values of the transfer coefficient  $\alpha$  are similar whether obtained from  $\partial E_p/\partial \log \nu$ ,  $E_p - E_{p/2}$ , or convolution analysis (vide infra); the significance of these values will be discussed later. In contrast, compounds **7** and **8** appear to be under mixed kinetic control:  $\partial E_p/\partial \log \nu$  falls between the expected values for a rate-limiting chemical step (30 mV/decade) and that for rate-limiting electron-transfer (60 mV/decade, for  $\alpha = 0.5$ ).

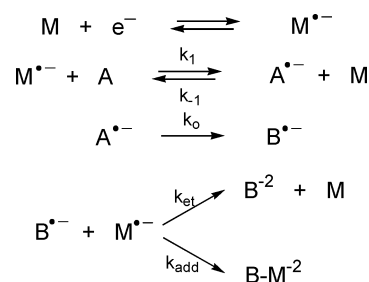
The voltammograms were subjected to convolution analysis; for **5**, electrode fouling was particularly problematic at low scan rates, so data analysis was restricted to experiments in the 600–1000 mV/s regime. For **6**, solvent/electrolyte discharge clearly distorted both the conventional and convolution voltammograms, complicating the determination of  $I_{lim}$ . For this system,  $I_{lim}$  was obtained by fitting the  $I$  vs  $E$  curves to a sigmoidal function, as described by Maran et al.<sup>35,36</sup> Convolution voltammograms for **5** and **6** are provided in the Supporting Information.

Plots of  $E$  vs the current function  $\ln((I_{lim} - I)/i(t))$  in accordance with eq 3 yields  $\alpha = 0.43$  and  $0.49$ , for **5** and **6**, respectively. Through application of eq 4, heterogeneous rate constants for electron transfer were determined as a function of electrode potential; a double-layer correction was not applied to the data. The  $\ln(k_{het})$  vs  $E$  data were curve-fit, and first derivatives calculated (at ca. 10 mV intervals, depending on scan rate) using Table Curve 2D<sup>37</sup> and leading to plots revealing the potential dependence of  $\alpha$  (eq 5). In accordance with Marcus theory, these  $\alpha$ - $E$  plots were linear, and extrapolation to  $\alpha = 0.5$  (corresponding to  $\Delta G^\circ = 0$ ) allows an estimate of  $E^\circ$  (eq

6).<sup>38–41</sup> On this basis,  $E^\circ$  is estimated to be  $-2.47$  and  $-2.89$  V, for **5** and **6**, respectively. Pertinent plots are provided in the Supporting Information.

$$\alpha = \frac{1}{2} + \frac{F}{8\Delta G_o^\ddagger} (E - E^\circ) \quad (6)$$

**Indirect Electrochemistry.** With indirect electrochemical methods (i.e., homogeneous redox catalysis),<sup>42–46</sup> an electron-transfer mediator or catalyst **M** rather than substrate **A** is reduced at the electrode surface (Scheme 3). For this to occur, the mediator must be more easily reduced than the substrate, (i.e., the peak potential of the substrate must be more positive than  $E^\circ_{M/M^{\bullet-}}$ ), and the reduction of **M** must be reversible. Reduction of the substrate occurs in solution (homogeneous) via electron transfer from the reduced form of the mediator ( $M^{\bullet-}$ ). Effects of substrate addition on the **M/M<sup>•-</sup>** couple are manifested experimentally by an increase in peak current and a loss of reversibility (if catalysis is occurring.) Kinetic control may be governed by either the homogeneous electron-transfer step ( $k_1$ ) or the chemical step ( $k_o$ , Scheme 3.) If the rate of the chemical step is faster than back electron transfer ( $k_o > k_{-1} [M]$ ), then the electron-transfer step is rate-limiting and  $k_1$  can be determined.

**Scheme 3**

If the chemical step is slow relative to back electron transfer ( $k_o < k_{-1} [M]$ ), the chemical step is rate-limiting with the electron-transfer step as a rapid pre-equilibrium. Under these conditions, the composite rate constant  $k_{obs} = k_o k_1 / k_{-1} = k_o K_1$  can be determined; if the reduction potential of the substrate ( $E^\circ_{A/A^{\bullet-}}$ ) is known,  $k_o$  can be extracted through application of eq 7.

$$\log K_1 = -F \left( \frac{E^\circ_{M/M^{\bullet-}} - E^\circ_{A/A^{\bullet-}}}{2.303RT} \right) \quad (7)$$

The key experimental observable in this method is the ratio of the voltammetric peak current of the mediator in the presence and absence of substrate ( $i_p/i_{pd}$ ) at a particular value of  $\gamma$  (the ratio of substrate to mediator concentration). Elucidation of the

(35) Donkers, R. L.; Maran, F.; Wayner, D. D. M.; Workentin, M. *J. Am. Chem. Soc.* **1999**, *121*, 7239–7248.

(36) Antonello, S.; Maran, F. *J. Am. Chem. Soc.* **1998**, *120*, 5713–5722.

(37) *TableCurve 2D*, 3.0 ed.; Jandel Scientific Software: San Rafael, CA.

(38) Antonello, S.; Benassi, R.; Gavioli, G.; Taddei, F.; Maran, F. *J. Am. Chem. Soc.* **2002**, *124*, 7529–7538.

(39) Antonello, S.; Maran, F. *J. Am. Chem. Soc.* **1997**, *119*, 12595–12600.

(40) Antonello, S.; Maran, F. *J. Am. Chem. Soc.* **1999**, *121*, 9668–9676.

(41) Donkers, R. L.; Workentin, M. S. *J. Phys. Chem. B* **1998**, *102*, 4061–4063.

(42) Andrieux, C. P.; Blocman, C.; Dumas-Bouchiat, J. M.; M'Halla, F.; Savéant, J. M. *J. Electroanal. Chem.* **1980**, *113*, 19–40.

(43) Andrieux, C. P.; Hapiot, P.; Savéant, J.-M. *Chem. Rev.* **1990**, *90*, 723–738.

(44) Andrieux, C. P.; Savéant, J.-M. *J. Electroanal. Chem.* **1986**, *205*, 43–59.

(45) Nadjo, L.; Savéant, J. M.; Su, K. B. *J. Electroanal. Chem.* **1985**, *196*, 23–34.

(46) Savéant, J. M.; Su, K. B. *J. Electroanal. Chem.* **1985**, *196*, 1–22.

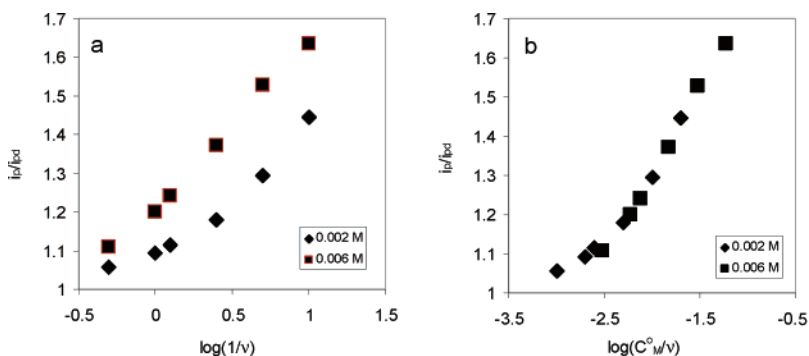


**Figure 3.** Mediated reduction of 1,2-diacetylcyclopropane (**5**) by 9-phenylanthracene (DMF, GCE, 0.5 M TBAP,  $\nu = 0.1 - 2.0$  V/s,  $\gamma = 1$ ).

**Table 2.** Rate Constants for Homogeneous Electron Transfer ( $k_1$ ) between the Reduced Form of the Mediator ( $\mathbf{M}^{\bullet-}$ ) and 1,2-Diacetylcyclopropane (**5**)

mediator (M)	$E^{\circ}_{\mathbf{M}/\mathbf{M}^{\bullet-}}$ <sup>a</sup>	$k_1$ ( $\text{M}^{-1}\text{s}^{-1}$ )	$\rho$
benzo[a]pyrene	-2.227	$1.85 \times 10^2$	0.00
9,10-diphenylanthracene	-2.253	$4.41 \times 10^2$	0.00
9-phenylanthracene	-2.292	$1.29 \times 10^3$	0.10
anthracene	-2.340	$3.43 \times 10^3$	0.00
9,10-dimethylanthracene	-2.342	$6.56 \times 10^3$	0.15
9-methylanthracene	-2.359	$4.32 \times 10^3$	0.00
$E^{\circ}_{\mathbf{A}/\mathbf{A}^{\bullet-}}$ <sup>a,b</sup>		$-2.62 \pm 0.21$	
$\lambda$ (kcal/mol) <sup>b</sup>		$25 \pm 5$	

<sup>a</sup> Volts vs 0.1 M  $\text{AgNO}_3/\text{Ag}$ . <sup>b</sup> Estimated on the basis of Marcus theory and eq 8.

rate-limiting step is straightforward because, at a given scan rate and  $\gamma$ ,  $i_p/i_{pd}$  varies with substrate concentration if electron transfer is rate-limiting.<sup>42–46</sup> This point is illustrated in Figure 3a for the mediated reduction of **5** with 9-phenylanthracene: A plot of  $i_p/i_{pd}$  vs  $\log(1/\nu)$  at two different concentrations yields two discrete lines. When substrate concentration is corrected for (i.e., a plot of  $i_p/i_{pd}$  vs  $\log(C^{\circ}_M/\nu)$ ; Figure 3b), the data points merge to form a single curve. These plots graphically demonstrate that homogeneous electron transfer is the rate-limiting step. Fitting of the data to appropriate working curves<sup>42–46</sup> as described previously<sup>13,14</sup> yields the rate constant for electron transfer between the substrate and  $\mathbf{M}^{\bullet-}$ . It should be noted that the kinetics of these systems are also complicated by a competing bimolecular reaction between  $\mathbf{M}^{\bullet-}$  and the ring-opened product  $\mathbf{B}^{\bullet-}$  involving addition ( $k_{\text{add}}$ ) and a second electron transfer ( $k_{\text{et}}$ ) which is accounted for in the working curves (Scheme 3). The parameter  $\rho$  is the rate constant ratio  $k_{\text{et}}/(k_{\text{add}} + k_{\text{et}})$ .<sup>45</sup>

For the reduction of **5** and **6** studied using several mediators, electron transfer was found to be rate-limiting in every instance using the diagnostic criteria described above. The results are summarized in Tables 2 and 3; pertinent plots are provided in the Supporting Information.

The reduction potential of the substrate ( $E^{\circ}_{\mathbf{A}/\mathbf{A}^{\bullet-}}$ ) was estimated using a Marcus-based treatment involving a non-linear least-squares fitting of  $k_1$  as a function of the reduction potential of the mediator ( $E^{\circ}_{\mathbf{M}/\mathbf{M}^{\bullet-}}$ ) according to eq 8,<sup>47</sup> (with  $K_d = 0.16 \text{ M}^{-1}$  and  $Z = 6 \times 10^{11} \text{ s}^{-1}$ ) as described previously.<sup>13,14</sup>  $\Delta G^{\circ}$  is the free energy change for the reaction  $\mathbf{M}^{\bullet-} + \mathbf{A} \rightarrow \mathbf{M} + \mathbf{A}^{\bullet-}$ , and is related to  $k_1$ ,  $k_{-1}$ , and the redox potentials of **A** and **M** according to eq 7. (Note: For **6**, the

**Table 3.** Rate Constants for Homogeneous Electron Transfer ( $k_1$ ) between the Reduced Form of the Mediator ( $\mathbf{M}^{\bullet-}$ ) and 1-Acetyl-2-phenylcyclopropane (**6**)

mediator (M)	$E^{\circ}_{\mathbf{M}/\mathbf{M}^{\bullet-}}$ <sup>a</sup>	$k_1$ ( $\text{M}^{-1}\text{s}^{-1}$ )	$\rho$
methyl benzoate	-2.623	$1.20 \times 10^2$	0.90
ethyl benzoate	-2.644	$2.00 \times 10^2$	0.90
benzonitrile	-2.688	$1.30 \times 10^2$	0.50
methyl 2-methylbenzoate	-2.692	$4.40 \times 10^3$	0.60
2-tolunitrile	-2.728	$1.29 \times 10^4$	0.35
$E^{\circ}_{\mathbf{A}/\mathbf{A}^{\bullet-}}$ <sup>a</sup>		$-3.07 \pm 0.06^b$	

<sup>a</sup> Volts vs 0.1 M  $\text{AgNO}_3/\text{Ag}$ . <sup>b</sup> Estimated on the basis of Marcus theory and eq 8.

data points were in the counter-diffusion-controlled region<sup>43,47</sup> of the Marcus plot (i.e., the third term of eq 8 dominates) and a reliable value of the reorganization energy ( $\lambda$ ) could not be obtained). Values of  $E^{\circ}$  obtained in this manner were consistent with, though slightly lower than, those obtained via convolution analysis.

$$\frac{1}{k_1} = \frac{1}{k_d} + \frac{1}{K_d Z \exp\left[\frac{-\lambda}{4RT} (1 + \Delta G^{\circ}/\lambda)^2\right]} + \frac{1}{k_d \exp(-\Delta G^{\circ}/RT)} \quad (8)$$

Terephthalonitrile proved to be an effective catalyst for the mediated reduction of **8**, and mixed kinetic control was observed. A procedure outlined by Savéant,<sup>48,49</sup> plotting  $1/k_{\text{app}}$  vs mediator concentration in accord with eq 9 (where  $k_{\text{app}}$  is the apparent rate constant assuming rate-limiting electron transfer), allowed the pertinent rate constants to be resolved:  $k_1 = 4.68 \times 10^6 \text{ M}^{-1} \text{ s}^{-1}$  and  $k_0 = 7.14 \times 10^5 \text{ s}^{-1}$ .

$$\frac{1}{k_{\text{app}}} = \frac{1}{k_1} + 0.33 \left( \frac{k_{-1}}{k_1 k_0} \right) C^{\circ}_M \quad (9)$$

Reconciliation of these results with the LSV results, which also were subject to mixed kinetic control, allowed this system to be solved completely. In Figure 4, the simultaneous variation of peak potential ( $E_p$ ) and peak width ( $E_p - E_{p2}$ ) as a function of sweep rate ( $\nu$ ) are reconciled to theoretical working curves (assuming  $\alpha = 0.5$ ) via the floating parameters  $C_1$  and  $C_2$ , defined in eqs 10 and 11,<sup>50</sup> with  $C_1 = -0.4778 \text{ V}$  and  $C_2 =$

(47) Ebersson, L. *Electron Transfer Reactions in Organic Chemistry*; Springer-Verlag: Berlin, 1987; Vol. 25.

(48) Amatore, C.; Combella, C.; Pinson, J.; Oturan, M. A.; Robveille, S.; Savéant, J.-M.; Thiébaud, A. *J. Am. Chem. Soc.* **1985**, *107*, 4846–4853.

(49) Andrieux, C. P.; Combella, C.; Kanoufi, F.; Savéant, J.-M.; Thiébaud, A. *J. Am. Chem. Soc.* **1997**, *119*, 9527–9540.

(50) Andrieux, C. P.; Savéant, J.-M.; Tallec, A.; Tardivel, R.; Tardy, C. *J. Am. Chem. Soc.* **1997**, *119*, 2420–2429.

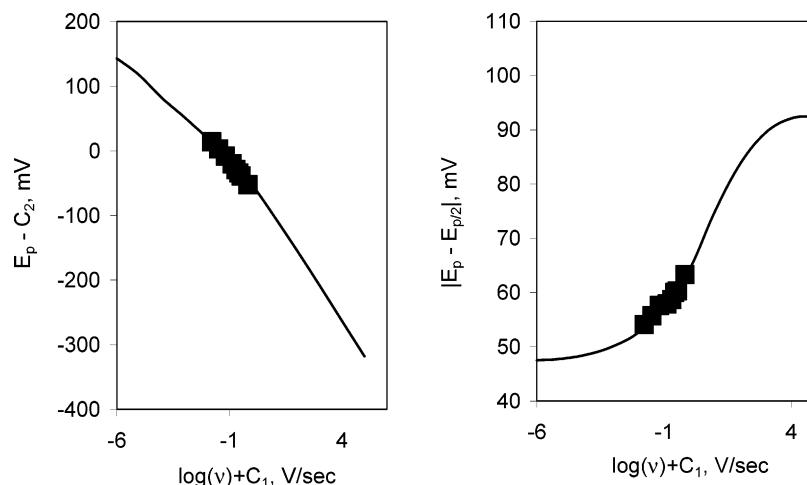


**Figure 4.** Variation of  $E_p$  and  $E_p - E_{p/2}$  as a function of sweep rate for the reduction of **8**. Solid lines represent theoretical working curves.

−1.949 V. Because  $k_o$  is now known (from the homogeneous redox catalysis experiments), eqs 10 and 11 can be combined to give eq 12. On this basis,  $E^\circ$  for **8** was determined to be −2.07 V.

$$C_1 = \log\left(\frac{F}{2RT} \frac{k_o D^2}{k_s^4}\right) \quad (10)$$

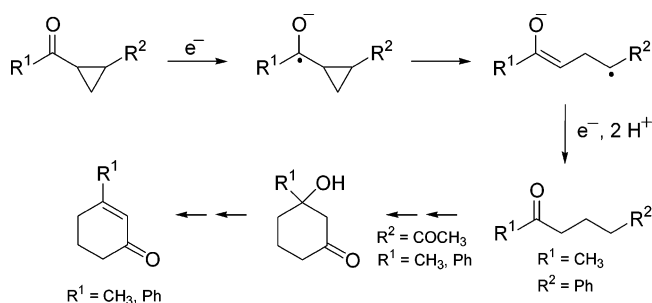
$$C_2 = E^\circ + \left(\frac{RT}{F} \ln 10\right) \log\left(\frac{k_o D}{k_s^2}\right) \quad (11)$$

$$E^\circ = C_2 - \frac{RT \ln 10}{2F} \left(\log k_o + C_1 - \log \frac{F}{2RT}\right) \quad (12)$$

For **7**, the mediated reduction could be achieved with terephthalonitrile ( $E^\circ_{MM^-} = -1.949$  V) and ring opening was rate-limiting with  $k_{obs} = (k_1/k_{-1})k_o = 10.6$  s<sup>−1</sup>. Fitting of the LSV results to the mixed kinetic control model as described above yielded  $C_1 = 3.163$  V and  $C_2 = -1.931$  V. Reconciling eq 12 with  $k_{obs}$  yields  $E^\circ = -2.13$  V and  $k_o = 1.0 \times 10^5$  s<sup>−1</sup>.

**Product Studies.** As expected, preparative scale electrolyses of **5** → **7** (constant potential, two electrons transferred) gave rise solely to cyclopropane ring-opened products. In the case of **5** and **7**, the initially produced diketone products underwent further reaction (Robinson annulation), presumably under the basic conditions associated with the electrolysis, or upon workup to yield cyclohexenones; the products and presumed mechanism for their formation are summarized in Scheme 4.

**Scheme 4**



In contrast, the product arising from the bulk electrolysis of **8** is remarkable and deserves further comment. In a process which is *catalytic* in electrons (<0.2 equiv of electrons transferred), constant current electrolysis of **8** (30 mA) yielded furan **12** in 65% isolated yield. The proposed mechanism for this reaction is the chain reaction depicted in Scheme 5, involving ring opening of **8**<sup>•−</sup>, subsequent cyclization of distonic radical ion **9**<sup>•−</sup> (in a Δ<sup>5</sup>-hexenyl manner), and electron transfer from **10**<sup>•−</sup> to **8** to complete the chain. Air oxidation of dihydrofuran **11** during workup produces **12**. The electron transfer from **10**<sup>•−</sup> to **8** should be favorable, as the reduction potential of dihydrofuran **11** is expected to be similar to other Ph(C=O)-containing compounds, ca. −2.2 V. (Furan **12** exhibits a reversible reduction wave with  $E^\circ = -2.00$  V, more positive because of the extended conjugation afforded by the furan ring). As noted, on a preparative scale, this reaction is catalytic in electrons. However, the voltammetry of **8** (see Figure 2) gave no indication of an electron-transfer catalyzed process; the observed currents were consistent with a two-electron process, suggesting that ring-opened radical anion **9**<sup>•−</sup> is simply reduced to the dianion under these conditions.

The transformation **8** → **11** is essentially a radical anion variant of the electron-transfer catalyzed “vinylcyclopropane → cyclopentene rearrangement.”<sup>51</sup> The intramolecular reaction between an enolate and enoyl radical (**9**<sup>•−</sup> → **10**<sup>•−</sup>) has also been previously proposed by Bauld et al.<sup>52</sup> to account for an unusual reduction of tethered bis(enones) to produce Diels–Alder-type product (**15**<sup>•−</sup> → **16**<sup>•−</sup>, Scheme 6).

## Discussion

**Cyclopropyl Ketones: LUMO Energies and Properties.** Calculations at the Hartree Fock 6-311G\* level were performed on compounds **5** → **8**, as well as numerous other cyclopropyl ketones for which reduction potentials have been previously

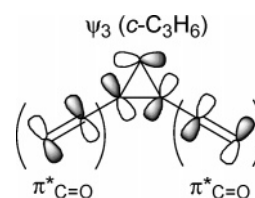
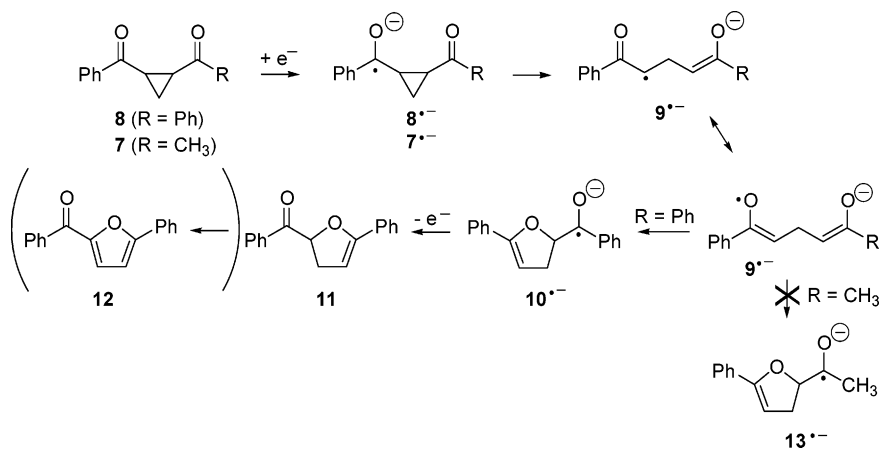
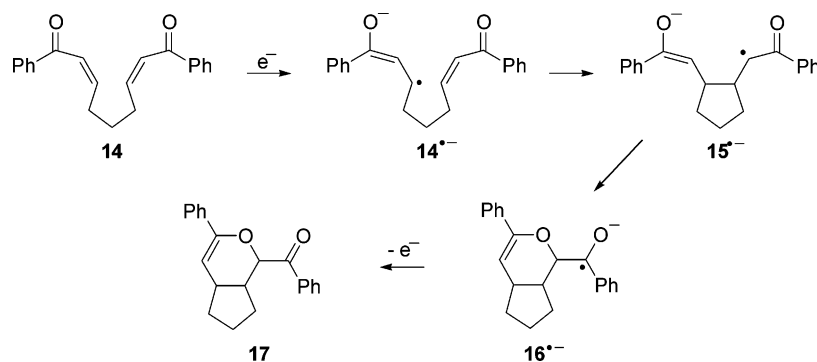


**Figure 5.** LUMO of cyclopropyl ketones **5**, **7**, and **8**.

Scheme 5



Scheme 6



reported. (A list of these compounds, their reduction potentials, and LUMO energies are available in the Supporting Information for this paper). Inspection of the LUMO indicates that for **5**, **7**, and **8**, the LUMO is derived from the two  $\pi^*$  C=O of the carbonyl groups, and the p-orbital-based LUMO of cyclopropane ( $\psi_3$ , Figure 1) as illustrated below in Figure 5. This analysis suggests that the corresponding radical anions of **5**  $\rightarrow$  **8** might be highly delocalized, and in the case of **5**, **7**, and **8**, charge and spin may be delocalized over both carbonyl groups through the cyclopropyl group.

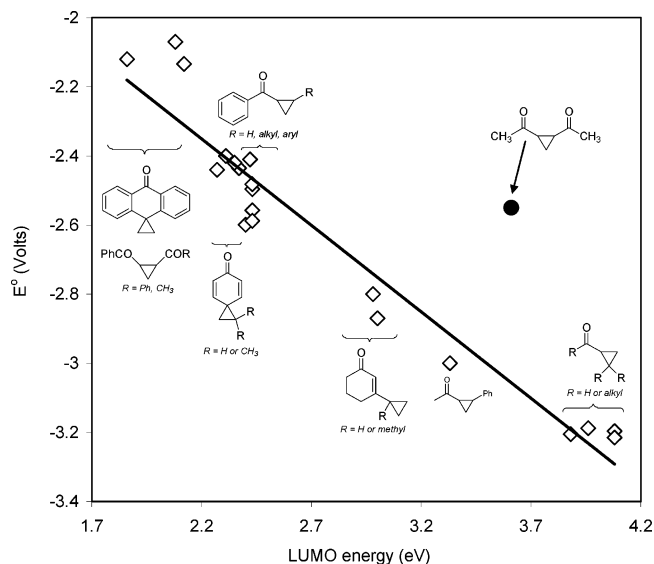
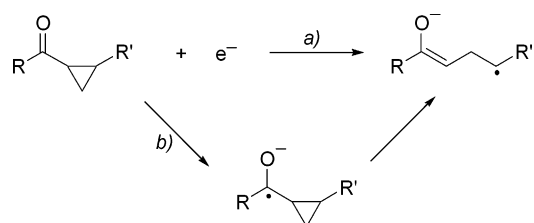


**Figure 6.** Observed reduction potentials vs  $E_{\text{LUMO}}$  (HF/6-311G\*) for cyclopropyl ketones.

Figure 6 presents a plot of the reduction potential of these compounds vs the calculated LUMO energy. The observed correlation suggests that, for most substrates, the LUMO energies of the neutral ketones are a reasonable predictor of reduction potential. It is noteworthy, however, that **5** shows the greatest deviation from the line and is about 400 mV more easily reduced than expected on the basis of its LUMO energy. (This point is addressed in more detail later).

Scheme 7



**DET: Concerted or Stepwise?** A fundamental question in modern electron transfer theory in situations where electron transfer and bond cleavage occurs is whether the two events occur simultaneously or in a stepwise manner.<sup>53–55</sup> For the reduction of cyclopropyl ketones, this point is illustrated in Scheme 7 where path (a) is the concerted pathway, and path (b) is stepwise. Only in the latter scenario does the radical anion exist as a discrete intermediate.

(51) Dinnocenzo, J. P.; Conlon, D. A. *J. Am. Chem. Soc.* **1988**, *110*, 2324–2326.

(52) Roh, Y.; Jang, H.-Y.; Lynch, V.; Bauld, N. L.; Krische, M. *J. Org. Lett.* **2002**, *4*, 611–613.

(53) Savéant, J. M. *Acc. Chem. Res.* **1993**, *26*, 455–461.

(54) Savéant, J.-M. *Adv. Phys. Org. Chem.* **2000**, *35*, 117–192.



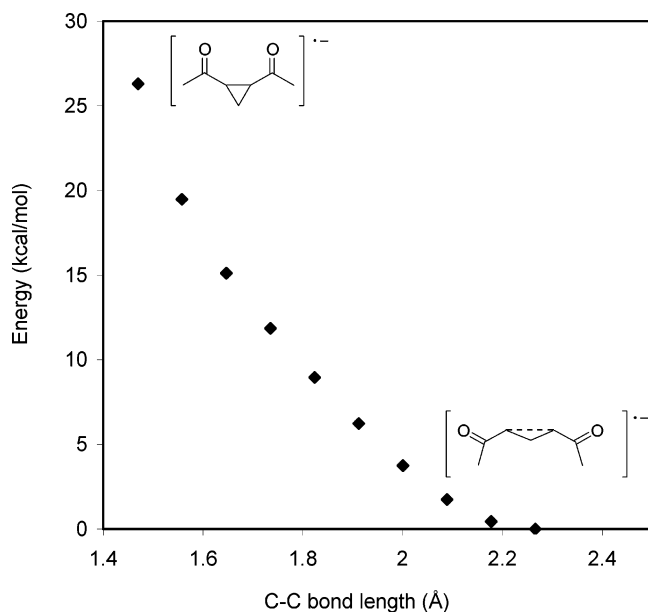


**Figure 7.** Energy of 1,2-diacetylcyclopropane radical anion ( $5^{\bullet-}$ ) as a function of C1–C2 distance, calculated at the UHF/6-31+G\* level.

The issues of radical anion structure, charge/spin delocalization, and the possibility of concerted DET were probed by performing molecular orbital calculations on the ring-closed and ring-opened radical anions derived from **5** → **8**. All of these calculations were performed at the UHF/6-31+G\* level; for **6** → **8**, spin contamination proved problematic, so the energies were obtained from a single-point ROHF calculation, using the UHF-derived geometries. It should be mentioned that the results at these levels of theory were significantly different from what was obtained from density functional calculations (B3LYP/6-31+G\*), which predict that both the ring-closed and ring-opened forms of symmetrical radical anions such as **5** and **8** are fully delocalized. In 1996, Bally noted that DFT calculations fail to accurately predict the dissociative behavior of symmetrical radical ions.<sup>56</sup> Accordingly, HF methods were used in this study because they do not seem to suffer from this problem.

At the UHF/6-31+G\* level, we were unable to locate a stationary structure corresponding to the cyclopropane ring-closed form of  $5^{\bullet-}$ . The only structure obtained was a cyclopropane ring-opened structure, with a C1–C2 bond length of about 2.5 Å, as opposed to the 1.5 Å normally associated with a cyclopropyl C–C bond. Attempts to map out the potential energy surface, by incrementally closing the C1–C2 bond revealed that the interaction between C1 and C2 was purely repulsive (Figure 7). Thus, the calculations very much suggest that  $5^{\bullet-}$  has no significant lifetime and that electron transfer to **5** may occur simultaneously with ring opening.

In contrast, the cyclopropane ring-closed forms of the radical anions generated from **6**, **7**, and **8** all reside at potential energy minima. Ring opening of  $6^{\bullet-}$  is highly exothermic, and the calculated barrier for ring opening is small, <1 kcal/mol. This result is certainly consistent with the fact that both the direct and indirect electrochemistry of **6** are characterized by rate-limiting electron transfer (suggesting a rate constant for ring opening  $\gg 10^7$  s<sup>-1</sup>).

The calculated barriers for ring opening of  $7^{\bullet-}$  and  $8^{\bullet-}$  are 7.7 and 6.1 kcal/mol, respectively, consistent with experiment: The rate constant for ring opening of  $8^{\bullet-}$  is about 1 order of magnitude greater than that for  $7^{\bullet-}$ . The calculations also provide insight into why  $7^{\bullet-}$  does not undergo the “vinylcyclopropane → cyclopentene-type rearrangement” depicted in Scheme 5. The calculations suggest that the distonic, ring-opened radical anion  $9^{\bullet-}$  (formed from  $7^{\bullet-}$ ) has the negative charge on the acetyl moiety. As a consequence, cyclized product **13** $^{\bullet-}$  does not enjoy the same resonance stabilization afforded to **10** $^{\bullet-}$  (formed by the cyclization of  $8^{\bullet-}$ ).

**Does 5 Fit Known Theoretical Models for Concerted DET?** At first glance, no. In principle, the question of concerted vs stepwise DET can be addressed by considering the voltammetric behavior of the substrates. Specifically, when the electron transfer is rate-limiting, the electron-transfer coefficient ( $\alpha$ ) is a sensitive diagnostic probe of mechanism. The electron-transfer coefficient is directly related, in the context of Marcus theory (eq 13), to the intrinsic barrier ( $\Delta G_o^\ddagger$ , the free energy barrier at zero driving force) for the electron transfer (eq 14). If bond breaking is occurring in the transition state, as would be the case for a concerted pathway, considerable structural reorganization is occurring (i.e., high intrinsic barrier) and  $\alpha$  is characteristically low (<0.5).<sup>38–40,57–67</sup>

$$\Delta G^\ddagger = \Delta G_o^\ddagger \left( 1 + \frac{\Delta G^\circ}{4\Delta G_o^\ddagger} \right)^2 \quad (13)$$

$$\alpha = \frac{\partial \Delta G^\ddagger}{\partial \Delta G^\circ} = \frac{1}{2} \left( 1 + \frac{\Delta G^\circ}{4\Delta G_o^\ddagger} \right) \quad (14)$$

For **5** and **6**,  $\alpha$  values obtained three different ways are summarized in Table 1. While electron transfer is rate-limiting in both cases, the derived  $\alpha$  values for **5** are slightly less than 0.5 but certainly not as low as is often found for a concerted dissociative electron-transfer process. In contrast, for **6**,  $\alpha = 0.5$  is consistent with a stepwise pathway, and certainly all the results for **7** and **8** clearly indicate electron transfer and ring opening occur in discrete steps and the corresponding radical anions have a finite lifetime (path (b), Scheme 7). The longer lifetime for  $7^{\bullet-}$  and  $8^{\bullet-}$  can clearly be attributed to resonance stabilization provided by the benzoyl group in the latter (Scheme 8).

Returning to the question of concerted DET for **5**. According to Marcus theory, the free energy of activation for electron transfer ( $\Delta G^\ddagger$ ) as a function of driving force ( $\Delta G^\circ$ ) is described by eq 13, where  $\Delta G_o^\ddagger = (\lambda_i + \lambda_o)/4$ ;  $\lambda_i$  and  $\lambda_o$  represent the

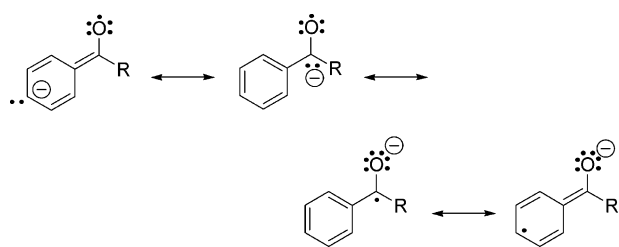
- (57) Andrieux, C. P.; Gallardo, I.; Savéant, J.-M.; Su, K.-B. *J. Am. Chem. Soc.* **1986**, *108*, 638–647.  
 (58) Andrieux, C. P.; Robert, M.; Saeva, F. D.; Savéant, J.-M. *J. Am. Chem. Soc.* **1994**, *116*, 7864–7871.  
 (59) Andrieux, C. P.; Savéant, J.-M.; Tardy, C. *J. Am. Chem. Soc.* **1998**, *120*, 4167–4175.  
 (60) Borsari, M.; Dallari, D.; Fontanesi, C.; Gavioli, G.; Iarossi, D.; Piva, R.; Taddei, F. *J. Chem. Soc., Perkin Trans. 2* **1997**, 1839–1843.  
 (61) Cardinale, A.; Isse, A. A.; Gennaro, A.; Robert, M.; Savéant, J.-M. *J. Am. Chem. Soc.* **2002**, *124*, 13533–13539.  
 (62) Christensen, T. B.; Daasbjerg, K. *Acta Chem. Scand.* **1997**, *51*, 307–317.  
 (63) Daasbjerg, K.; Jensen, H.; Benassi, R.; Taddei, F.; Antonello, S.; Gennaro, A.; Maran, F. *J. Am. Chem. Soc.* **1999**, *121*, 1750–1751.  
 (64) Houmam, A.; Hamed, E. M.; Still, I. W. J. *J. Am. Chem. Soc.* **2003**, *125*, 7258–7265.  
 (65) Lexa, D.; Savéant, J.-M.; Schäfer, H. J.; Su, K.-B.; Vering, B.; Wang, D. L. *J. Am. Chem. Soc.* **1990**, *112*, 6162–6177.  
 (66) Workentin, M. S.; Donkers, R. L. *J. Am. Chem. Soc.* **1998**, *120*, 2664–2665.  
 (67) Workentin, M. S.; Maran, F.; Wayner, D. D. M. *J. Am. Chem. Soc.* **1995**, *117*, 2120–2121.

(55) Maran, F.; Workentin, M. S. *Interface* **2002**, 44–49.

(56) Bally, T.; Sastry, G. N. *J. Phys. Chem. A* **1997**, *101*, 7923–7925.



Scheme 8



inner and outer reorganization energies. The heterogeneous rate constants obtained from the convolution analysis of **5** and **6** can be treated in the context of Marcus theory through the Eyring equation (eq 15), where  $Z$  for heterogeneous electron transfer is obtained from eq 16 ( $k_B$  is Boltzmann's constant;  $m$  is the molecular mass). The results of this analysis are provided in Figure 8, and described below.

$$\Delta G^\ddagger = -\frac{RT}{F} \ln\left(\frac{k_{\text{het}}}{Z}\right) \quad (15)$$

$$Z_{\text{echem}} = \left(\frac{k_B T}{2\pi m}\right)^{1/2} \quad (16)$$

Fitting the heterogeneous kinetic data for the reduction of **5** and **6** to eq 13 leads to reorganization energies ( $\lambda$ ) = 1.49 and 1.32 eV, respectively. If it is assumed that **6** undergoes stepwise electron transfer, then the reorganization energy for **5** is only 0.17 eV (4 kcal/mol) higher, and at first glance, this small difference is difficult to rationalize with a concerted DET process for **5**.

Savéant has developed theory<sup>53,54,68</sup> pertaining to concerted DET where an additional term is added to the inner reorganization energy to account for the strength of the bond ( $D_R$ ) which is cleaved during electron transfer;  $\Delta G_o^\ddagger = (D_R + \lambda_o)/4$ . Because **6** undergoes stepwise electron transfer, inferring little or no bond-breaking occurs in the transition state, it may be reasonable to assume that most of  $\lambda$  is attributable to solvent reorganization ( $\lambda_o$ ). In DMF, the solvent reorganization energy can be estimated by  $\lambda_o$  (eV) =  $3/a$  (Å), where  $a$  is the radius of the electron acceptor.<sup>69</sup> Assuming that this radius can be approximated by the size of the  $\text{CH}_3\text{CO}$  group in **6** (i.e., the charge is localized as indicated by the MO calculations) leads to an estimated  $\lambda_o$  of 1.27 eV, very close to the observed value of 1.32 eV.

On this basis, the characteristics of the  $\ln(k_{\text{het}})$  vs  $\Delta G^\circ$  plot for **5** can be constructed on the basis of concerted DET theory. The C1–C2 bond strength of **5** is estimated to be 45 kcal/mol (1.95 eV), based upon the hypothetical hydrogenation reaction depicted in eq 17, using literature values for strengths of the H–H bond and C–H bonds, and  $\Delta H_f^\circ$ 's obtained via DFT calculations (B3LYP/6-31G\*) as described previously.<sup>13</sup> This estimate of the C–C bond strength for **5** is quite reasonable on the basis of group additivity. The C–C bond strength in ethane is 90 kcal/mol, vs 84 kcal/mol for acetone,<sup>70</sup> suggesting a radical

(68) Savéant, J. M. In *Advances in Electron Transfer Chemistry*; Mariano, P. S., Ed.; JAI Press: Greenwich, 1994; Vol. 4, pp 53–116.

(69) Pause, L.; Robert, M.; Savéant, J.-M. *J. Am. Chem. Soc.* **2001**, *123*, 11908–11916.

(70) Kerr, J. A. In *Handbook of Chemistry and Physics*, 84th ed.; CRC Press: Boca Raton, FL, 2003–2004; pp 9-52–9-75.

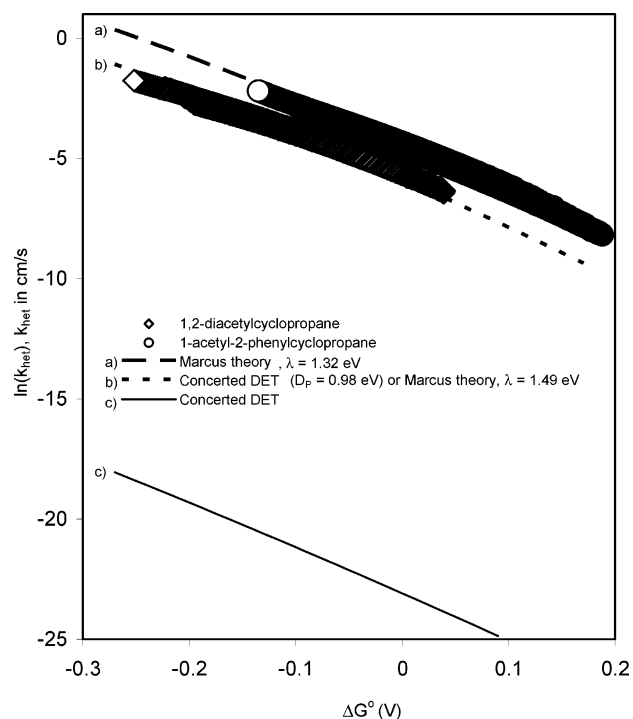
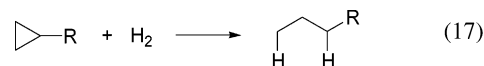


**Figure 8.** Plots of  $\ln(k_{\text{het}})$  vs  $\Delta G^\circ$  for the reduction of 1,2-diacetylcyclopropane (**5**) and 1-acetyl-2-phenylcyclopropane (**6**) reconciled to electron transfer theory.

stabilization energy of ca. 6 kcal/mol for  $\text{CH}_3(\text{C}=\text{O})$ . The C–C bond strength in cyclopropane is 61 kcal/mol,<sup>71</sup> two  $\text{CH}_3(\text{C}=\text{O})$



groups would lower this to 49 kcal/mol, reasonably consistent with the DFT approach.

The assumption that  $\lambda_o$  for **5** is the same for as for **6** and that  $D_R = 1.95$  eV leads to the solid (bottom) curve in Figure 7 clearly showing that the activation/driving force relationship for **5** does *not* fit the concerted DET model.

The concerted DET model assumes there is no significant interaction between the radical and anion after bond cleavage. However, coulombic interactions have been detected in some systems<sup>38,61,64,72–78</sup> and are the result of attractive anion–dipole interactions between the negatively charged leaving group and neutral radical. These interactions have the net effect of offsetting the importance of the  $D_R$  term because, in essence, the bond is not completely broken. This situation is illustrated in Figure 9, where concerted DET to R–X results in a ( $\text{R}^+\text{X}^-$ ) caged pair, which subsequently diffuses apart to the free radical

(71) Berson, J. A.; Pedersen, L. D.; Carpenter, B. K. *J. Am. Chem. Soc.* **1976**, *98*, 122–143.

(72) Pause, L.; Robert, M.; Savéant, J.-M. *J. Am. Chem. Soc.* **2000**, *122*, 9829–9835.

(73) Costentin, C.; Robert, M.; Savéant, J.-M. *J. Am. Chem. Soc.* **2003**, *125*, 10729–10739.

(74) Chang, J.; Goddard, J. D.; Houmam, A. *J. Am. Chem. Soc.* **2004**, *126*, 8076–8077.

(75) Costentin, C.; Robert, M.; Savéant, J.-M. *J. Am. Chem. Soc.* **2004**, *2004*, 16834–16840.

(76) Isse, A. A.; Gennaro, A. *J. Phys. Chem. A* **2004**, *108*, 4180–4186.

(77) Costentin, C.; Louault, C.; Robert, M.; Teillout, A.-L. *J. Phys. Chem. A* **2005**, *109*, 2984–2990.

(78) Costentin, C.; Robert, M.; Savéant, J.-M. *J. Am. Chem. Soc.* **2003**, *125*, 105–112.

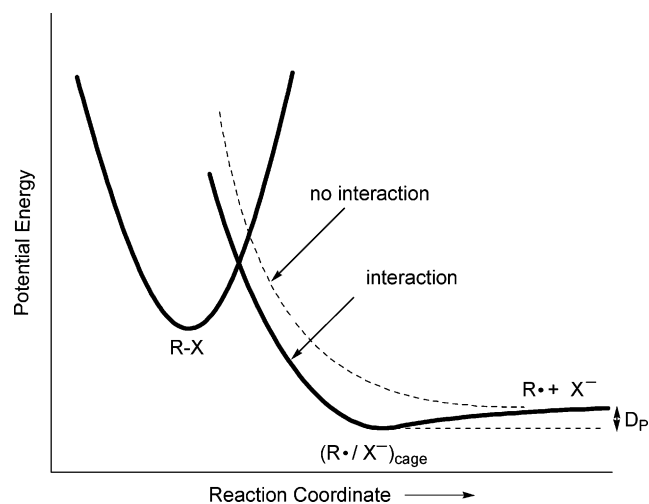


**Figure 9.** Concerted dissociative electron transfer to R–X with and without interaction between the products R• and X<sup>−</sup>.

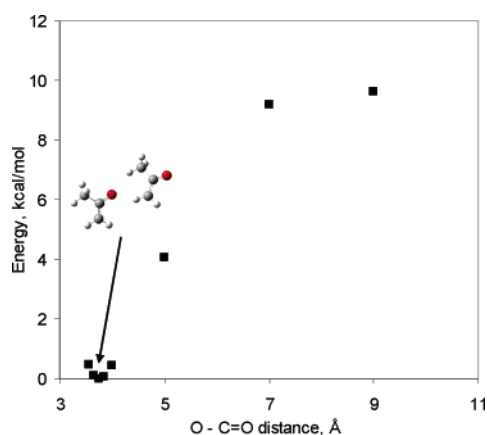


**Figure 10.** Energy of CH<sub>3</sub>(CO)CH<sub>2</sub><sup>−</sup>/CH<sub>3</sub>(CO)CH<sub>2</sub>• as a function of the distance between the enolate oxygen and carbonyl carbon of the enoyl radical.

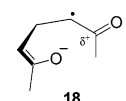
and anion. In this situation, eq 18 pertains where  $D_P$  refers to the magnitude of the interaction between the fragments, and the  $\Delta G_{SP}^\circ$  term refers to the difference between the standard free energies of the separated and caged products (mainly attributable to entropy).<sup>72</sup>

$$\Delta G^\ddagger = \frac{(\sqrt{D_R} - \sqrt{D_P})^2 + \lambda_o}{4} \left[ 1 + \frac{\Delta G^\circ - \Delta G_{SP}^\circ}{(\sqrt{D_R} - \sqrt{D_P})^2 + \lambda_o} \right]^2 \quad (18)$$

In **5**, an anion/dipole interaction may be occurring between the enolate anion portion and the C=O group of the enoyl radical portion of the distonic radical anion, illustrated with **18**. In applying the “sticky” concerted DET model to this system (eq 18), we assume  $\Delta G_{SP}^\circ \approx 0$  because for these cyclopropane cleavages, the radical and anion fragments cannot diffuse apart because they are tethered by the CH<sub>2</sub> group. While the experimental results for **5** can be fit to the “sticky” concerted DET model (dotted line in Figure 7), the magnitude of the interaction ( $D_P = 0.98 \text{ eV} = 23 \text{ kcal/mol}$ ) seems unreasonably high.

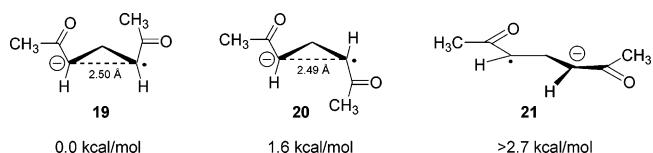
To verify this conjecture, potential interactions between an enolate anion (CH<sub>3</sub>COCH<sub>2</sub><sup>−</sup>) and enoyl radical (CH<sub>3</sub>COCH<sub>2</sub>•), analogous to that proposed in structure **18** were probed

computationally. An energy minimum (no imaginary frequencies) was found for a structure which placed the oxygen of the enolate anion  $\sim 3.75 \text{ \AA}$  from the carbonyl carbon of the enoyl radical. In Figure 10, energy is plotted as a function of the distance between these two atoms, suggesting an interaction energy around 9.6 kcal/mol (0.42 eV) in the gas phase. It is expected that the magnitude of this interaction would be reduced in DMF solvent and in the presence of electrolyte. In addition, the ring-opened form of **5**<sup>•−</sup> does not appear to have the flexibility to achieve a conformation such as that depicted in structure **18**, which would allow the enolate oxygen to directly interact with the carbonyl group. Thus, although the results seem to fit the “sticky” concerted DET model, the derived value of  $D_P = 0.98 \text{ eV}$  is completely unreasonable.



**Does **5** Relax to a “Loose” Radical/Anion Pair Upon Addition of an Electron?** In some ways, the results observed for the reduction of **5** are reminiscent of those presented for the one-electron reduction of various disulfides (RSSR) by Maran et al. In these cases,  $\alpha$  was low, indicative of a larger than normal intrinsic barrier to electron transfer. For the disulfides, it was suggested that electron transfer occurred concurrently with a lengthening of the S–S bond to form a loose radical/ion pair (RS<sup>•−</sup>/SR), and the large intrinsic barrier to electron transfer is interpreted as arising from this structural reorganization. In essence, the bond is not completely ruptured, and a similar argument might explain the kinetics of the reduction of **5**.

To address this issue, the structure of the ring-opened (distonic) radical anion was probed further (UHF/6-31+G\*). The lowest energy structure for this species finds the two CHCOCH<sub>3</sub> groups of the enolate and enoyl radical parallel to each other, with the CH's separated by  $\sim 2.5 \text{ \AA}$ ; “cisoid” form **19** is lower in energy than “transoid” **20**. The geometric and electronic structure of the ring-opened radical anion is not consistent with the characterization of this structure as a loose radical/ion pair: The distance between the two CHs is identical to the distance between C1 and C3 of propane, which is obviously “ring-opened.” Moreover, the radical anion is not delocalized (i.e., most of the negative charge is localized on one of the CHCOCH<sub>3</sub> groups, and most of the spin on the other.) It is interesting to note that other conformations such as **21**, which in principle suffer from less torsional strain, are higher in energy and do not exist at potential energy minima, and this may indicate an (small) ion–dipole interaction between the enolate and enoyl portions of the radical ion.



**One-Electron Reduction of **5**: Resolution of the Dichotomy?** As discussed, MO calculations suggest **5**<sup>•−</sup> does not exist as a discrete intermediate, yet the kinetic results for the reduction of **5** fit neither the normal nor “sticky” concerted DET

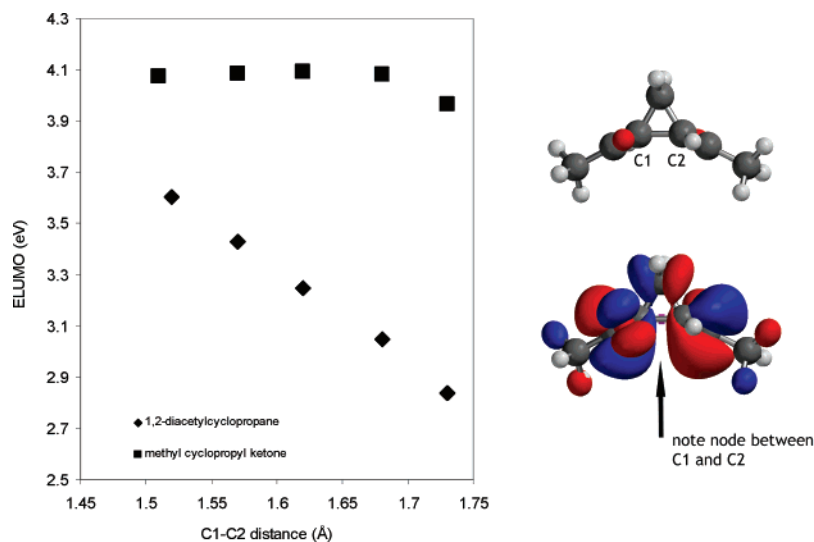


**Figure 11.** Variation in the energy of the LUMOs for 1,2-diacetylcyclopropane (**5**) and methyl cyclopropyl ketone (**22**) as a function of C1–C2 distance; the LUMO of **5**.

models—assuming that **5** has the same solvent reorganization energy as **6** and is localized. The geometric and electronic structure of the (distonic) ring-opened radical anion is not consistent with a relaxed C–C bond, as might be anticipated for a loose radical/anion pair-type structure, as has been suggested for reduction of RSSR. Rather, the kinetic results fit rather well with the classical Marcus model, with a reorganization energy ( $\lambda$ ) only slightly (0.17 eV) higher than for compound **6**—which, consistent with both theory and experiment, certainly undergoes stepwise DET (electron transfer followed by ring opening).

The conflicting results obtained for **5** may be rationalized by considering the unique bonding properties of the cyclopropyl group. As noted earlier (Figure 5), the LUMO of **5** is derived from the two  $\pi^*$  orbitals of C=O, and the p-orbital-based LUMO of the cyclopropyl group. Calculations indicate that the LUMO energy of **5** is *very* sensitive to C–C bond length, much more so than is the case for methyl cyclopropyl ketone (**22**). For both these compounds, stretching the C–C bond from 1.5 Å (normal cyclopropyl C–C bond length) to 1.7 Å “costs” the same—about 9 kcal/mol (0.39 eV). However, while the LUMO energy of **22** does not change significantly over this range, the LUMO energy of **5** decreases dramatically (from 3.6 to 2.8 eV) as the bond is lengthened. This observation makes sense because there is a significant antibonding interaction between C1 and C2 in the LUMO of **5** (Figure 11).

With classical Marcus theory, the internal component of the reorganization energy encompasses geometric distortions needed to bring the LUMO energy close to the energy of the donor so that electron transfer can occur. In the case of **5**, a 0.2 Å lengthening of the C1–C3 bond may be sufficient to do this, and at little cost (ca. 9 kcal/mol or 0.39 eV) in the context of internal reorganization energy ( $\lambda_i$ ). (Perhaps not so coincidentally, this geometric distortion would be sufficient to bring **5** back onto the line in the plot of  $E^\circ$  vs LUMO energy for the various cyclopropyl ketones, Figure 6). Also, since the LUMO encompasses both carbonyl groups and the cyclopropane, the effective size of the electron acceptor is larger than for a simple cyclopropyl ketone (i.e., the charge is transferred to a more delocalized system). Assuming that the radius can be ap-

proximated by the size of the O=C–CH–CH–C=O framework, then the estimated solvent reorganization energy in DMF ( $\lambda_o = 3/a$ , where  $a$  is the radius in Å of the acceptor) is 1.07 eV. It is somewhat satisfying to note that the total reorganization energy  $\lambda = \lambda_i + \lambda_o$  based upon this analysis (1.46 eV) is close to the experimentally observed value of 1.49 eV.

Finally, does electron transfer theory need to be modified to accommodate these results? Probably not. The estimate of 0.39 eV for the internal reorganization energy associated with the reduction of **5** is approaching one-fourth of the estimated strength of the C1–C2 bond strength, as predicted by the Savéant concerted DET model. Indeed, refitting the kinetic data to this model (again using  $D_R = 1.95$  eV) and solving for the solvent reorganization energy leads to  $\lambda_o = 1.01$  eV—close to the estimated value of 1.07 eV, assuming electron transfer to a more delocalized system. Given the uncertainties associated with the experimental data, the nature of some of these assumptions, and the number of parameters involved (and their compensatory relationship), it is probably unwise to attach too much quantitative significance to these values. However, qualitatively at least, the experimental results for the reduction of **5** can be accommodated by the concerted DET model, and the resulting parameters are of reasonable magnitude.

## Conclusions

The one-electron reduction of **5** may proceed via a concerted DET process; however, the only evidence for this statement is derived from the results of MO calculations. The reorganization energy obtained from experiment is only slightly higher than expected on the basis of the behavior of other cyclopropyl ketones and at first glance, is consistent with a normal (stepwise) electron-transfer process. However, the MO calculations also suggest that a low reorganization energy may be quite reasonable for the reduction of this compound: A modest, “low-cost” internal reorganization (lengthening of the C1–C2 bond) may occur which lowers the LUMO energy sufficiently for electron transfer to occur; the estimated total reorganization energy based upon this hypothesis (assuming a more delocalized structure, consistent with the properties of the LUMO) matches well with experiment. The energetic consequences of this internal reor-

ganization are also of the magnitude predicted by the concerted DET model, again, with the assumption of a more delocalized structure. Thus, what makes this possible case of concerted DET particularly difficult to detect from an experimental standpoint is that two compensating factors are at play: The onset of concerted DET raises the internal reorganization energy, but that is offset by a lower solvent reorganization associated with formation of a more delocalized system (compared to other cyclopropyl ketones). We suspect that the reason that this sort of issue has not come up previously is that well-documented examples of concerted DET involve electron transfer to a rather localized framework, typically a  $\sigma^*$  antibonding orbital.

In contrast, the radical anion of **6** exists for a finite lifetime, and hence, stepwise DET is observed. However, the barrier to ring opening is very small. Substituents at the 2-position of methyl cyclopropyl ketones play a critical role in determining whether the DET will be concerted vs stepwise. It seems likely that additional examples of concerted DET may be found in these (and related) systems, but for the reasons discussed, the unambiguous experimental detection of concerted vs stepwise DET will be problematic.

For **7** and **8**, a stepwise mechanism is preferred, and the rate constant for ring opening of the corresponding radical anions is lower. The difference is clearly attributable to the resonance stabilization afforded by the benzoyl group for the radical anions generated from **7** and **8**.

Cyclopropyl ring openings and fragmentations of this type are often used as mechanistic probes for electron transfer. The fact that **5** may undergo concerted dissociated electron transfer, and **6**<sup>-</sup> has a very low barrier for ring opening, means that

these compounds are truly "hypersensitive" mechanistic probes. Finally, although an unsubstituted cyclopropyl group does not stabilize a radical anion, electron-withdrawing substituents at C2 significantly enhance the electron-withdrawing properties of the cyclopropyl group. The energy of the LUMO of the neutral ketone is (in general) a good predictor of the reduction potential of these compounds. (The exception is **5**, whose reduction potential is more favorable than predicted, possibly because concerted DET is operative and the reduction is partly driven by the relief of cyclopropane ring strain.) There is no evidence which suggests that **6**<sup>-</sup>, **7**<sup>-</sup>, or **8**<sup>-</sup> are fully delocalized (symmetrically, in their ring-closed forms) through the cyclopropyl group, as might be predicted on the basis of the properties of the LUMO of the neutral ketone.

**Acknowledgment.** Financial support from the National Science Foundation (CHE-0108907) and (CHE-0548129) is acknowledged and appreciated. We also thank Profs. Mark Anderson, Paul Carlier, T. Daniel Crawford, and Diego Troya for enlightening and helpful discussions which aided us in the preparation of this manuscript and several anonymous reviewers whose helpful comments and criticisms proved invaluable in the evolution of this manuscript.

**Supporting Information Available:** Voltammetry data and plots pertaining to the electrochemistry of **5**–**8**, table of reduction potentials and LUMO energies of several cyclopropyl-containing ketones used to construct Figure 6, the full Gaussian '03 citation, and absolute energies and optimized geometries of all calculated structures. This material is available free of charge via the Internet at <http://pubs.acs.org>.

JA063857Q